Bioconjugate Chemistry

Article

pubs.acs.org/bc

Differential Polymer Structure Tunes Mechanism of Cellular Uptake and Transfection Routes of Poly(β-amino ester) Polyplexes in Human Breast Cancer Cells

Jayoung Kim,[†,‡] Joel C. Sunshine,[†,‡] and Jordan J. Green*[,†,‡,§]

[†]Department of Biomedical Engineering and the Translational Tissue Engineering Center and [§]Department of Ophthalmology, Johns Hopkins University School of Medicine, Baltimore, Maryland 21231, United States

[‡]The Institute for Nanobiotechnology, Johns Hopkins University, Baltimore, Maryland 21218, United States

Supporting Information

ABSTRACT: Successful gene delivery with nonviral particles has several barriers, including cellular uptake, endosomal escape, and nuclear transport. Understanding the mechanisms behind these steps is critical to enhancing the effectiveness of gene delivery. Polyplexes formed with poly(β-amino ester)s (PBAEs) have been shown to effectively transfer DNA to various cell types, but the mechanism of their cellular uptake has not been identified. This is the first study to evaluate the uptake mechanism of PBAE polyplexes and the dependence of cellular uptake on the end group and molecular weight of the polymer. We synthesized three different analogues of PBAEs with the same base polymer poly(1,4-butanediol diacrylate-*co*-4-amino-1-butanol) (B4S4) but with small changes in the end group or molecular weight. We quantified the uptake and transfection efficiencies of the pDNA polyplexes formulated from these polymers in hard-to-transfect triple negative human breast cancer cells (MDA-MB 231). All polymers formed positively charged (10−17 mV) nanoparticles of ∼200 nm in size. Cellular internalization of all three formulations was inhibited the most (60−90% decrease in cellular uptake) by blocking caveolae-mediated endocytosis. Greater inhibition was shown with polymers that had a 1-(3-aminopropyl)-4-methylpiperazine end group (E7) than the others with a 2-(3-aminopropylamino)-ethanol end group (E6) or higher molecular weight. However, caveolae-mediated endocytosis was generally not as efficient as clathrin-mediated endocytosis in leading to transfection. These findings indicate that PBAE polyplexes can be used to transfect triple negative human breast cancer cells and that small changes to the same base polymer can modulate their cellular uptake and transfection routes.

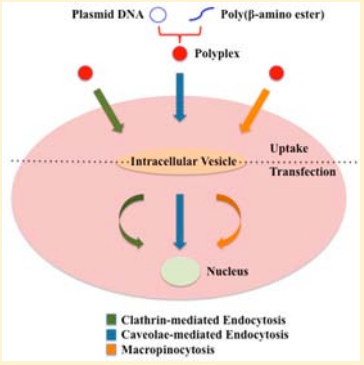

INTRODUCTION

Genetic abnormality is responsible for a wide range of human diseases including cancer. Gene therapy holds great promise in treating cancer because the gene product can be chosen to cause cell death in cancer cells while being benign to healthy cells. Despite the promising utility, advances in technology have been limited due to the difficulty in finding delivery vectors with and optimal balance between safety and efficacy.[1] Certain recombinant viral vectors take advantage of the evolutionary ability of viruses to efficiently insert DNA cargo into cells, but pose challenges with limited cargo size, difficulty in manufacturing, and safety concerning immunogenicity and tumorigenicity.[2,3]

Nonviral delivery vehicles have been developed to address these limitations. Cationic polymers such as poly(β-amino esters) (PBAE) and poly(ethylenimine) (PEI) are such nonviral vectors that exhibit significant advantages in manufacture, cargo capacity, and biocompatibility.[4] Cationic polymers, such as PBAEs bind negatively charged DNA via electrostatic interactions to form stable nanoparticles or "polyplexes" with low cytotoxicity.[5] Past studies have shown that PBAE nanoparticles can overcome critical barriers to gene delivery, which include cellular uptake across the cell membrane, endosomal escape via the "proton sponge" effect, and cytosolic plasmid release.[6]

There are three major, endocytic pathways by which cells take up foreign materials: clathrin-mediated endocytosis, (CME) caveolae-mediated endocytosis (CvME), and macropinocytosis.[7] CME occurs from clathrin-coated pits on the plasma membrane as ligands bind to transmembrane receptors.[8] The coated pits of about 100−150 nm in diameter can form a polygonal clathrin lattice with adaptor proteins, and are eventually pinched off from the plasma membrane. These internalized vesicles sequentially form early endosomes, late endosomes, and finally lysosomes.[9] Chlorpromazine, which is known to translocate clathrin and adaptor proteins from the plasma membrane to intracellular vesicles, has been used in previous studies to inhibit CME.[10] Caveolae-mediated uptake is characterized by flask-shaped invaginations of the plasma membrane that are 50−100 nm in diameter.[11] Caveolin, a

Received: May 18, 2013
Revised: October 21, 2013
Published: December 9, 2013

dimeric protein, binds cholesterol and forms a striated coat on the surface of the plasma membrane invagination it creates.[7] Dynamin II is believed to be responsible for budding off of caveolae,[12] and its transient recruitment to the site depends on the activation of tyrosine kinase.[13] Many reports confirm that genistein, a tyrosine kinase inhibitor, blocks CvME.[11] Macropinocytosis describes nonspecific engulfment of extracellular fluid into large endocytic vehicles called macropinosomes.[14] The creation of membrane ruffling requires intracellular signaling by rho-family GTPases and phosphoinositide-3-kinase (PI3K), and is thus blocked by PI3K inhibitor, wortmannin.[15]

It is important to elucidate how biomaterial design can enhance cellular uptake and transfection efficacy. New cancer therapies are needed for difficult-to-treat cancers, such as "triple-negative" breast cancer (TNBC), as Her2, the estrogen receptor, and the progesterone receptor, are not expressed, and therefore the most effective drugs in the anti-breast cancer armamentarium cannot be used. This manuscript examines the cellular uptake of PBAE polyplexes in human TNBC cells (MDA-MB 231) through parallel routes and how differential structure can tune the route of cellular uptake. The relative contribution of different routes of cellular entry for successful transfection for PBAE polyplexes is also investigated.

EXPERIMENTAL PROCEDURES

Cell Culture. The human breast cancer MDA-MB231 cells were first synchronized for their cell cycle stage by incubation in Dulbecco's modified Eagle medium (DMEM) with L-glutamine (DMEM 11965, Invitrogen, Carlsbad, CA) supplemented with 1% penicillin/streptomycin but no fetal bovine serum (FBS) for 24 h. Following synchronization, cells were incubated in DMEM with 10% FBS and 1% penicillin/streptomycin. Cells were grown under a humid 5% CO_2 atm at 37 °C.

Materials. 1,4-Butanediol diacrylate (B4), 1,6-hexanediol diacrylate (B6), 4-amino-1-butanol (S4), 5-amino-1-pentanol (S5), and 1-(3-aminopropyl)-4-methyl-piperazine (E7) (Alfar Aesar, Ward Hill, MA), 1,3-propanediol diacrylate (B3), 1,5-pentanediol diacrylate (B5) (Monomer-Polymer and Dajac Laboratoris, Trevose, PA), 2-methyl-1,5-diaminopentane (E4) (TCI America, Portland, OR), 2-(3-aminopropylamino)ethanol (E6), and branched 25 kDa poly(ethylenimine) (PEI) (Sigma-Aldrich, St. Louis, MO) were purchased and used as received. EGFP-N1 DNA (Elim Biopharmaceuticals, Hayward, CA), Label IT-Tracker Cy3 kit (Mirus Bio LLC, Madison, WI), chlorpromazine hydrochloride (Sigma), genistein (Sigma), wortmannin (Sigma), FITC-conjugated cholera toxin subunit B (Sigma), fluorescein-conjugated human transferrin (Life Technologies, Carlsbad, CA), and CellTiter 96 AQueous One MTS assay (Promega, Fitchburg, WI) were obtained from commercial vendors and used per manufacturer's instructions.

Polymer Synthesis and Characterization. A combinatorial array of poly(β-amino ester) (PBAE) polymers was obtained by a two-step polymer synthesis procedure. As an example, acrylate-terminated poly(1,4-butanediol diacrylate-*co*-4-amino-1-butanol) base polymer (B4S4) was first synthesized at 1.2:1 acrylate:amine monomer molar ratio by adding 1.82 g of B4 (9.2 mmol) to 0.68 g of S4 (7.6 mmol) in a glass vial without any solvent and reacting them in the dark under magnetic stirring for 24 h at 90 °C. In the second step, the diacrylate-terminated base polymers were end-capped with amine-containing small molecules 2-(3-aminopropylamino)-ethanol (E6) and 1-(3-aminopropyl)-4-methyl-piperazine (E7). 625 mg of polymer in 4 mL of THF was mixed with 4 mL of 0.5 M of end-capping amine solution in THF, which were then allowed to stir at 500 rpm overnight at room temperature. Following ether purification, the final polymers were dried and stored in DMSO at 100 mg/mL with desiccant at −20 °C until use. Polymer structure was characterized on a Bruker spectrometer by ^{1}H NMR spectroscopy (400 MHz, d_6-DMSO). Spectra for B4S4E6 and B4S4E7 are shown in Figure S1. Polymers were also analyzed for molecular weight by gel permeation chromatography using a Waters Breeze System and 3 Styragel Columns (7.8 × 300 mm) in series: HR 1, HR 3, and HR 4. The samples were run at 1 mL/min with 95% THF/5% DMSO/0.1 M piperidine eluent.

Particle Characterization. Particles were formulated in 25 mM sodium acetate buffer (pH = 5.0) for 60 ng/uL DNA at 60 w/w (equivalent to 70 N/P) ratio for PBAE/DNA polyplexes and 2 w/w (equivalent to 15 N/P ratio) for PEI/DNA polyplexes. Both dynamic light scattering (DLS) using a Malvern Zetasizer Nano ZS (Malvern Instruments, Malvern, U.K., detection angle 173°, 633 nm later) and nanoparticle tracking analysis (NTA) using a Nanosight NS500 (Amesbury, U.K., 532 nm laser) were used to determine particle size. Particles were diluted into 1× PBS (pH = 7.4) 5-fold for DLS and 50-fold for NTA. DLS reported intensity-weighted *Z*-averaged of the particle diameter in nm, while NTA reported number-weighted diameter upon analysis of the Brownian motion from a 60 s movie. Zeta potential was determined using a Malvern Zetasizer Nano ZS (Malvern Instruments, Malvern, U.K.) with samples diluted 15-fold into 1× PBS. The mean and standard error of the mean were calculated.

Uptake and Transfection. MDA-MB 231 cells were plated at a density of 15 000 cells/100 μL in clear CytoOne 96-well tissue culture plates (USA Scientific) in 100 μL media/well to allow for 24 h cell adhesion. For uptake experiments, eGFP pDNA was labeled with Cy3 using the Label IT Tracker kit, and diluted into 25 mM NaAc buffer (pH = 5) to a final concentration of 60 ng/μL. Polymer stock solutions at 100 mg/mL in DMSO were diluted to respective w/w ratios (i.e., 3.6 μg/μL for 60 w/w), and 45 μL of diluted polymers and diluted DNA were vigorously mixed in another 96-well plate with multichannel pipet. The particles were allowed to self-assemble for 10 min, following which 20 μL of nanoparticles was added to 100 μL of regular serum containing medium on the cells. For PEI polyplexes, eGFP pDNA diluted into 150 mM NaCl to 60 ng/μL was mixed with equal volume of PEI diluted to 120 ng/μL (2 w/w) in 150 mM NaCl from a stock solution at 1 mg/mL in dH_2O. Ten minutes after complexation, 20 μL of PEI/DNA polyplexes was added to 100 μL of medium on cells. Cells are incubated with polyplexes for four hours for both uptake analysis and transfection experiments in order to allow maximal uptake with minimal effect of exocytosis. The time dependence of polyplex uptake was investigated and found to increase linearly, as shown by Figure S2, and therefore the 4 h time point was used for all analysis. Four hours after transfection, the cells were washed twice with Heparin containing PBS (50 μg/mL), detached by 30 μL trypsin, added with 170 μL PBS containing 2% v/v FBS, centrifuged at 800 rpm at RT for 5 min, and resuspended in 40 μL after removing 160 μL supernatant for analysis by flow cytometry (Accuri C6 with HyperCyt high-throughput adaptor). For the three positive controls, fluorescein-labeled human transferrin, FITC-labeled cholera toxin subunit B, and FITC-labeled dextran, 10 μL were added to 100 μL of medium at 16 μg/mL, 1 μg/mL, and 1 mg/

dx.doi.org/10.1021/bc4002322 | *Bioconjugate Chem.* 2014, 25, 43−51

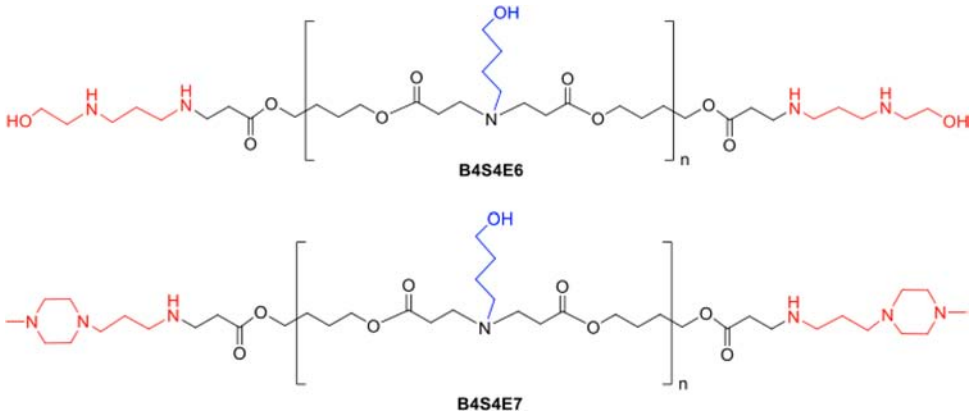

Figure 1. Structures of PBAEs. (A) B4S4E6 and (B) B4S4E7 have the same B4S4 base polymer but different end groups.

mL followed by 15 min, 5 min, and 30 min incubation, respectively. Cy3% positive is the percentage of total cells that are Cy3+ as measured by Cy3 labeled DNA by FACS. Cy3+ cells were gated by two-dimensional gating of FL1 vs FL2 using FlowJo 7.6.5 software. Only well measurements with greater than 500 cell counts were analyzed.

For transfection studies, the same protocol was followed as uptake experiments, except that after washing the cells 4 h post transfection, the cells were added with 100 μL of fresh media and incubated for additional 48 h before FACS analysis. Propidium iodide (Invitrogen, Carlsbad, CA) was added at 1:200 to the final 40 μL before FACS analysis to detect dead cells. GFP % positive is the percentage of total live cells (PI-negative cells) that are GFP+ as measured by expression of green fluorescent protein (GFP) from exogenously delivered DNA by FACS. PI− and GFP+ cells were sequentially gated for by two-dimensional gating of FL1 vs FL2. The percent decrease in uptake and transfection was normalized to each of the no-inhibitor control conditions and is indicated as pair coordinates for comparison between uptake and transfection.

Endocytosis Inhibition Study. The same uptake and transfection protocols were followed except that cells were incubated with endocytosis inhibition drugs for 1 h prior to transfection with polyplexes. Drugs were added by replacing medium with 100 μL fresh medium containing drugs at their respective concentrations. For optimization studies, chlorpromazine (28 μM, 35 μM, 42 μM, 56 μM, 70 μM), genistein (100 μM, 150 μM, 200 μM, 250 μM, 300 μM), and wortmannin (25 nM, 50 nM, 75 nM, 100 nM, 200 nM) were added to see the effective inhibiting concentrations. For this study, the optimized concentrations of 42 μM for chlorpromazine, 300 μM for genistein, and 200 nM for wortmannin were used.

Cell Viability Study. After normal transfection and washing, the cells were incubated for an additional 24 h in 100 μL of fresh medium. Cell viability was measured with CellTiter 96 AQueous One MTS assay. Cells were incubated at 37 °C for 1.5 h after addition of the CellTiter reagent at 20 μL/well and measured for absorbance at 490 nm using a plate reader (Synergy 2). The absorbance was normalized to untreated cells of each group after subtracting off background absorbance.

Statistical Analysis. All statistics were performed using the GraphPad Prism 5 software package. One-way ANOVA with Dunnett post-test was used to examine multiple comparisons within a single PBAE group. One-way ANOVA with Bonferroni post-test was used to compare data across multiple PBAE groups.

RESULTS AND DISCUSSION

Polymer Synthesis, Screening, and Characterization. Our group has extensively explored nonviral gene delivery to different cell lines in vitro using PBAEs to form polyplexes with negatively charged DNA[16−20] and siRNA.[21,22] PBAEs are important to study as they have been demonstrated to have virus-like efficacy in certain human primary cells and low cytotoxicity.[23] Some studies investigated how physical and chemical properties of PBAEs affect gene delivery efficacy.[24−26] More recently, Sunshine et al. concluded that polymer end-group structure alters overall cellular uptake and transfection in COS-7 cells.[27] However, the exact cellular uptake mechanisms of PBAE polyplexes and the specific dependence PBAE structural variants on cellular uptake have never been investigated. In this work we investigated, for three PBAE polymer analogues and for PEI as a control, the major route of cellular uptake, the cellular uptake route most responsible for transfection, and how these properties change with PBAE end-group and molecular weight.

A combinatorial array of PBAE polymers was synthesized using different monomers and small end-capping molecules shown in Figure S1A. The results of ^{1}H NMR on the key PBAEs investigated in this study, 446L, 447L, 447H, confirm the synthesis and structure (Figure S1B), and are comparable to the spectrum of PBAEs from previous literature.[26,28,29] We did not observe any side reactions, including transamidation or transesterification, under the experimental conditions.

This array of polymers was evaluated in MDA-MB 231 human breast cancer cells for general uptake and transfection efficiencies (Figure S3). Intriguingly, acrylate-terminated PBAEs showed no evident uptake or transfection regardless of base or side monomers used to form the polymers, while amine monomer end-capped PBAEs all showed uptake, although with variation in their efficiencies dependent on polymer structure. In general, B4 monomer (4 carbons between acrylate groups), which is more hydrophobic than B3 (3 carbons between acrylate groups) but less so than B5 (5 carbons between acrylate groups), resulted in higher uptake efficacy. In addition, PBAEs with end-group molecules E6 (2-(3-aminopropylamino)ethanol) and E7 (1-(3-aminopropyl)-4-methyl-piperazine) showed greater uptake than those with E4 (2-methyl-1,5-diaminopentane), with the exception of backbone polymers of B3S5 and B6S5. Transfection efficacy was the

dx.doi.org/10.1021/bc4002322 | Bioconjugate Chem. 2014, 25, 43−51

highest with B4 monomers, while relatively insensitive to side-chain monomer and end-group molecules. It appears that there is an optimal structure of linear PBAEs for uptake and transfection in MDA-MB231 cells: a base polymer with intermediate hydrophobicity (i.e., B4S4 and B4S5) and an end-cap molecule with additional secondary or tertiary amines. In order to study the effect of end-group in cellular uptake, B4S4E6 and B4S4E7 at 60 w/w, which yielded high uptake of 88% and 89% and transfection of 46% and 52%, respectively, were selected for further experiments. The structure of these two polymers is shown in Figure 1. Furthermore, two different batches of B4S4E7 with different molecular weights as determined by GPC were used to evaluate the effect of molecular weight on the cellular uptake pathway (Figure 2).

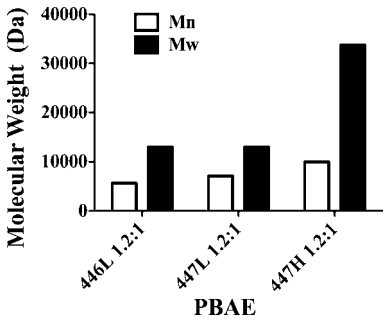

Figure 2. Polymer characterization. Molecular weights of PBAEs determined by gel permeation chromatography. Black bars represent weight-averaged molecular weight and white bars represent number-averaged molecular weight.

Low molecular weight B4S4E7 (447L) had a molecular weight of 13 kDa, which was the same as B4S4E6 (B4S4E6), while the high molecular weight version of B4S4E7 (447H) was 34 kDa, ensuring a significant difference in molecular weight.

Particle Characterization. As mentioned above, different endocytic pathways are initiated by invaginations or protrusions of the cell membrane of varying sizes. While clathrin-coated pits can be 100−150 nm in diameter, the size of caveolae is usually 50−100 nm.[8,11] Due to these physical restrictions, some groups have investigated size-dependent endocytosis. However, the observations from previous experiments in the literature show a discrepancy from these the biological descriptions on the sizes of these protrusions. For example, Rejman et al. showed that latex beads with a diameter of less than 200 nm enter cells mostly via clathrin-mediated endocytosis, whereas greater-sized beads up to 500 nm preferred caveolae as uptake mechanism.[30] The PBAE polyplexes formed by different polymer structures and used in the current study are verified to have a monodisperse size distribution, and their sizes by nanoparticle tracking analysis are also equivalent, without regard to specific polymer structure. This enables us to investigate the effect of polymer structure on cellular uptake mechanism without particle size being a confounding variable.

Previous literature also reports that positively charged particles are endocytosed through clathrin-dependent pathway, while uptake of negatively charged particles is independent of clathrin and caveolin.[31] Therefore, particle charge of PBAE polyplexes could potentially affect cellular entry as well.

In order to investigate particle size and charge as potential variables, we measured the hydrodynamic diameter and zeta potential of our PBAE nanoparticles. For sizing, both dynamic light scattering (DLS) and nanoparticle tracking analysis (NTA) methods were used. DLS gives an intensity-weighted hydrodynamic diameter that may skew measurement to larger-sized particles in polydisperse samples, whereas NTA measures number-averaged size to give a potentially more accurate evaluation of size distribution.[16,32] Figure 3A shows that while DLS measurements have a range of size between 200 and 300 nm, NTA measured all PBAE and PEI particle formulations to be similarly sized between 180 and 230 nm. All particles used in this study were also positively charged, as evaluated by Zetasizer with zeta potential ranging from +10 to +17 mV (Figure 3B). The similar nanoparticle size and zeta potential among these three PBAE polyplexes, which share the same base polymer structure but differ in polymer end-group and/or molecular weight, ensure that the observations in subsequent experiments are free from confounding factors of particle size and charge.

Optimization of Endocytosis Inhibitors. Past studies on cellular uptake have used various chemical molecules and methods to inhibit endocytic mechanisms. Chlorpromazine or potassium depletion is used to block CME, filipin, or genistein to inhibit CvME, and wortmannin or amiloride to prevent macropinocytosis.[33] However, in some cases, different concentrations of the same inhibitor were used in different cell lines. For example, one study used 28 μM chlorpromazine on HeLa cells while another treated 56 μM chlorpromazine on COS-7 cells.[34,35] This indicates that optimization of these inhibiting drugs is essential for a specific cell type. We determined the most efficient yet nontoxic concentrations of chlorpromazine, genistein, and wortmannin in MDA-MB 231 cells.

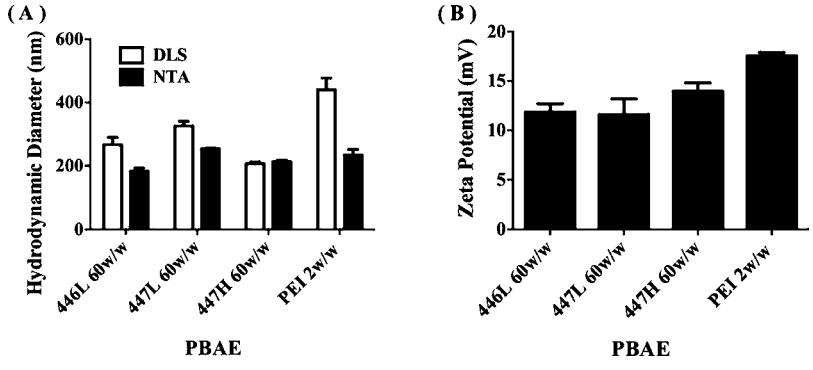

Figure 3. Particle characterizations. (A) Hydrodynamic diameter of nanoparticles measured using dynamic light scattering (white) and nanoparticle tracking analysis (black). (B) Zeta potential of nanoparticles. Data are mean ± SEM, n = 3.

dx.doi.org/10.1021/bc4002322 | *Bioconjugate Chem.* 2014, 25, 43−51

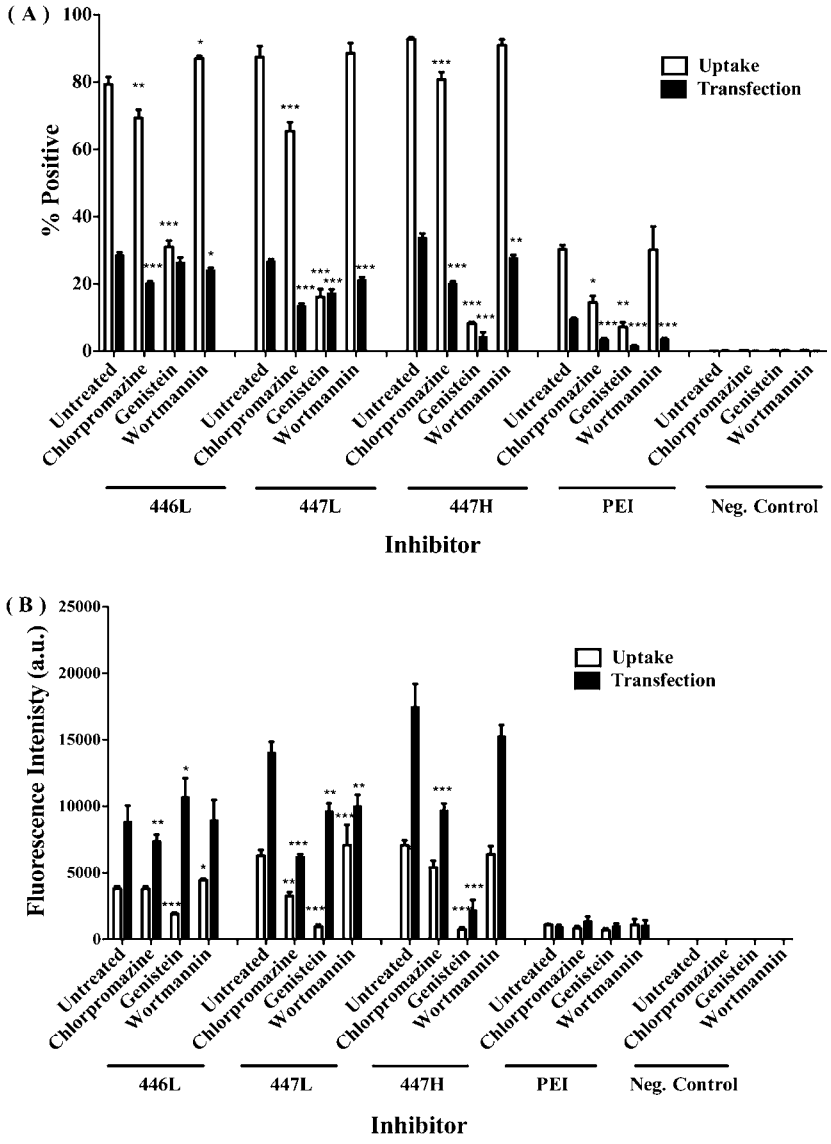

Figure 4. Effect of endocytosis inhibitors on PBAE gene delivery. Uptake (white) and transfection (black) efficacies are shown as (A) percentage of positive cells and (B) geometric mean of fluorescence intensity measured by flow cytometry. *X*-axis represents inhibitor-treated condition. Data are presented as mean ± SEM with $n \geq 4$. * Statistically significant decrease ($p < 0.05$) vs no-inhibitor control in each group.

Figure S3A-C shows uptake efficacy and cell viability upon preincubation with inhibitors and treatment with B4S4E6 polyplexes, PEI polyplexes, or positive controls. Chlorpromazine caused loss of cells during the washing step due to detachment from the adhering surface (data not shown), which led to decreased normalized metabolic activity of below 50% at 56 μM. We therefore optimized chlorpromazine concentration to 42 μM, at which it was functioning as a CME inhibitor to nanoparticles while maintaining cell viability above 90%. Genistein and wortmannin did not induce a loss of metabolic activity/cause cytotoxicity at the highest concentration tested, but showed complete inhibition of CvME and a partial effect on macropinocytosis, respectively. Hence, 300 μM genistein and 200 nM wortmannin were used in subsequent experiments. Some researchers have stated a concern regarding a possible lack of specificity with pharmacological inhibitors, and that the inhibitors may affect more than one endocytosis mechanism.[36] Hence, we tested the above inhibitors against positive controls. Human transferrin (hTr) is often reported as a positive control for CME, cholera toxin subunit B (CtxB) for CvME, and dextran for macropinocytosis.[37−39] Indeed, uptake of hTr was blocked by ∼40% specifically in response to chlorpromazine at 42 μM and was not inhibited by either genistein or wortmannin. CtxB uptake was inhibited by ∼40% specifically to genistein at 300 μM, and was not inhibited by either chlorpromazine or wortmannin. Likewise, dextran uptake was inhibited by 67% in response to wortmannin but was relatively insensitive to chlorpromazine and genistein (Figure S4D).

Effects of Inhibitors on Cellular Uptake and Transfection. We tested inhibition of cellular uptake and transfection of PBAE polyplexes with optimized concentrations of endocytosis blockers. All three formulations, B4S4E6 and B4S4E7 at the same lower molecular weight (446L and 447L) and B4S4E7 at higher molecular weight (447H), showed 80−90% uptake efficacy in the absence of inhibitors (Figure 4A). In all formulations, blocking CME decreased uptake efficacy to 70−90% compared to the no-inhibitor control, while inhibition of macropinocytosis did not affect uptake (Figure 4A, Table 1). However, uptake was significantly reduced to 40%, 20%, and 10% in 446L, 447L, and 447H, respectively, when CvME was

dx.doi.org/10.1021/bc4002322 | *Bioconjugate Chem.* 2014, 25, 43−51

Table 1. Normalized Uptake and Transfection Efficacy as a Function of Polymer Type and Cellular Uptake Inhibitors[a]

nanoparticle	chlorpromazine	genistein	wortmannin
446L 60 w/w	(13%, 29%)	(61%, 8%)	(−10%, 16%)
447L 60 w/w	(25%, 49%)	(83%, 35%)	(−1%, 20%)
447H 60 w/w	(13%, 40%)	(91%, 88%)	(2%, 18%)
PEI 2 w/w	(52%, 63%)	(71%, 84%)	(0%, 63%)

[a]Decrease in uptake and transfection efficiencies from endocytosis inhibition are normalized to each respective no-inhibitor control. Normalized values are indicated as pair coordinates (% decrease in uptake, % decrease in transfection) for side-by-side comparison.

inhibited. PEI polyplexes showed a similar trend in uptake mechanism, where the decrease in uptake was the most with genistein, less with chlorpromazine, and none with wortmannin. Hence, caveolae-mediated endocytosis was determined to be the major uptake pathway, and clathrin-mediated endocytosis a minor uptake pathway, for both PBAE and PEI nanoparticles. This is in agreement with previous studies that showed different polyplexes formed with cationic polymers, such as PLL-g-PEG, PEI, and pDMAEMA, were internalized mostly via CvME.[34,35,40]

Interestingly, the degree of PBAE polyplex uptake varied depending on small changes in the end-group and molecular weight even though the base polymer structure and nanoparticle size and zeta potential were essentially the same. 447L was more efficient in uptake via both CME and CvME pathways than 446L, and uptake of 447H was more concentrated in CvME than 447L. This result can be explained in part by a possible nanoparticle polydispersity, which is indicated by the difference in size from the number-averaged measurement (NTA) and the intensity-averaged measurement (DLS). Increased monodispersity is correlated to greater dependence on CvME as the major uptake pathway in the order 446L, 447L, and 447H.

PBAE formulations showed a different transfection profile upon endocytosis inhibition. 446L had a ∼30% decrease in transfection when CME was inhibited, while blocking of other pathways led to eGFP expression level comparable to control, even when it led to substantial decreases in uptake (for genistein, a 61% decrease in uptake only resulted in an 8% decrease in transfected cells) (Figure 4A, Table 1). The decrease in transfection in the presence of chlorpromazine closely matched the decrease in uptake. These data may indicate that, for 446L nanoparticles, clathrin-mediated uptake results in efficient gene expression in MDA-MB 231 cells, while caveolae-mediated uptake is a particularly inefficient pathway toward gene expression. For 447L, a drop of 49% and 35% in transfection was measured with chlorpromazine and genistein, respectively. Thus, the CvME uptake pathway was responsible for successful transfection of a greater fraction of 447L polyplexes than 446L polyplexes. However, CME still remained the most efficient uptake route leading to transfection (Table 1). 447H polyplexes had a significant 90% decreased transfection rate when caveolae was blocked, while inhibition of CME reduced transfection efficacy by 40%. Macropinocytosis was also responsible for ∼20% of the transfection in 447H. With higher molecular weight polymer, both CME and CvME resulted in the most efficient pathway to gene expression. In PEI polyplexes, transfection followed a similar inhibition trend as uptake with CvME as the most important pathway, which conforms to the findings by Rejman et al.[34]

Caveolae-mediated endocytosis gains greater importance in both uptake and transfection in MDA-MB 231 cells with the E7 end-group rather than the E6 end-group and at higher molecular weight PBAE. This may be explained by several possibilities. Different end-groups may lead to specific interactions with the cell membrane and its receptors that preferentially induce one uptake pathway over another. Downstream steps from cellular uptake, such as endosomal release and DNA unbinding, are also important for successful transfection, and the tertiary amines that are part of the E7 end group may play a role in these downstream steps following CvME.[27,41] This hypothesis is further supported by previous studies, which found that polyplexes formed from polymer consisting of primary amines, such as PLL-g-PEG, have poor transfection efficacy following their major uptake via CvME,[40] while tertiary amines in polymers such as PEI and pDMAEMA enhanced gene transfection via CvME.[34,35] Also, higher molecular weight PBAE may cause tighter binding to DNA[41,42] and this may help protect the DNA from premature degradation.

It is also important to note that similar results are observed when measuring successful transfection of GFP plasmid by either of the two metrics in this experiment: % positively transfected cells or geometric mean of fluorescence intensity (Figure 4B). Both plots follow similar trends for both uptake and transfection, and this is further supported by the positive, linear correlation between the values for % positive cells and the arithmetic mean of fluorescence intensity and % positive cells and the geometric mean of fluorescence intensity (Figure S5). This indicates that our findings are equally applicable on both a per cell basis and on a population of cells basis.

Effects of Combinations of Inhibitors. We further evaluated the most efficient uptake and transfection mechanisms by using combinations of inhibitors. Figure 5C shows that the use of multiple inhibitors in all combinations maintained cell viability above a 70% threshold. For uptake, all combinations except chlorpromazine and wortmannin caused nearly complete inhibition of uptake in all PBAE and PEI formulations (Figure 5A). In other words, the only condition in which CvME was functional allowed comparable uptake efficacy to no-inhibitor control. This result is in agreement with the single inhibitor drug findings above with caveolae as the major route of uptake for PBAE nanoparticles.

When treated with multiple inhibitors, the cellular uptake, as well as transfection, is reduced by greater magnitude as compared to equivalent single-inhibitor conditions. This seemingly "synergistic" effect can be explained by compensatory mechanism reported by Harush-Frenkel et al.[31] When one uptake pathway is blocked, other mechanisms become more aggressive to uptake foreign materials. Cells have less opportunity to compensate if multiple pathways are blocked simultaneously, hence showing lower level of uptake and transfection efficacies.

For transfection efficacy, a shift in the endocytosis pathway that leads to a higher transfection rate, which was observed in single-inhibitor study, was not observed in multiple-inhibitor experiments. Rather, all three PBAE formulations showed a similar trend. This could be explained by compensation for pathway blockade, forcing more particles through the unaffected mechanism. All PBAE nanoparticles had a significantly higher transfection rate when they entered cells via CvME at around 30% (Figure 5A). Transfection level for CME was highest for 447L at 12% and lowest for 447H at 6%,

dx.doi.org/10.1021/bc4002322 | Bioconjugate Chem. 2014, 25, 43−51

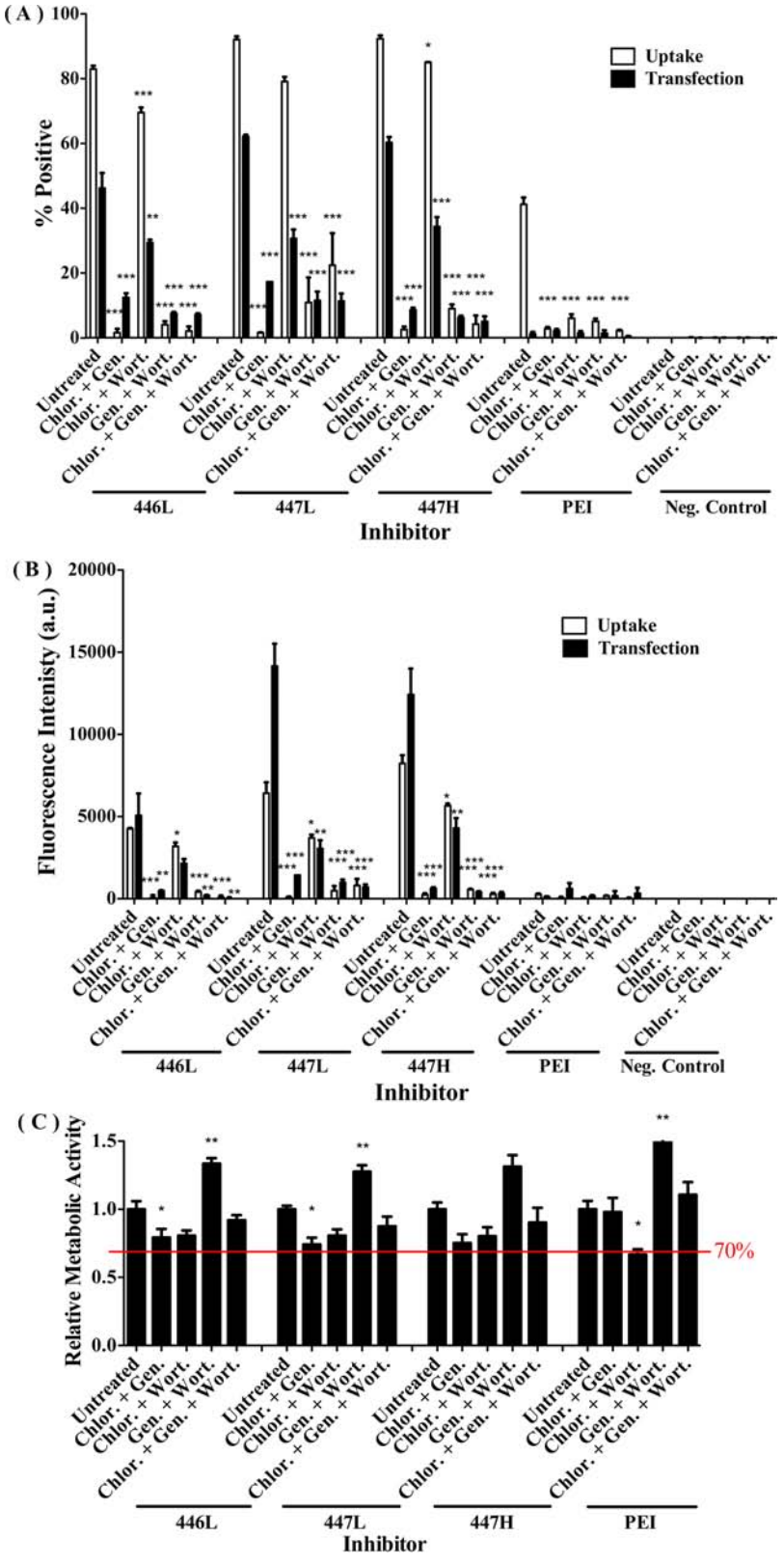

Figure 5. Combinations of cellular uptake inhibitors. Cellular uptake (white) and transfection (black) efficacies shown as (A) percentage of cells and (B) geometric mean of fluorescence intensity measured by flow cytometry. (C) Cell viability after simultaneous treatment of two or more inhibitors. *X*-axis represents inhibitor-treated condition. Data are presented as mean ± SEM with $n \geq 4$. * Statistically significant decrease ($p < 0.05$) vs no-inhibitor control in each group for both uptake/transfection and cell viability plots.

while that for macropinocytosis was around 15% for 446L and 447L and 8% for 447H. These results further confirm that CvME plays a major role in uptake and transfection. However, polyplexes that enter via CvME are less than 50% efficient in completing their path from uptake to transfection. CME facilitated the journey for most of the polyplexes it internalized

dx.doi.org/10.1021/bc4002322 | *Bioconjugate Chem.* 2014, 25, 43−51

from cellular uptake to successful transfection. In certain cases, as in 446L with both chlorpromazine and genistein, higher transfection was observed than uptake rate. This may be due to a lower fluorescence intensity of Cy3 labeled DNA than high expressing GFP in successfully transfected cells, as the flow cytometer may not have discriminated between cells with low frequency of uptake and cells which had higher background autofluorescence. Figure S6A-B supports this assessment as it illustrates that the shift in Cy3 fluorescence intensity is smaller than the shift in GFP fluorescence intensity. Because expression of exogenously delivered GFP DNA in highly transfected cells can result in fluorescence signal that is orders of magnitude above background, the geometric mean of fluorescence intensity is larger for transfection than it is for cellular uptake of labeled DNA (Figure 5B). The trends in cellular uptake and transfection are comparable between the % positive and the geometric mean of fluorescence intensity values.

CONCLUSIONS

PBAEs are cationic polymers that can be used to complex with negatively charged DNA to form polyplexes or nanoparticles. These polyplexes, specifically B4S4E6 and B4S4E7, can transfect triple-negative human breast cancer MDA-MB 231 cells with high efficacy (48% and 53%, respectively) and thus have the potential to be used in gene therapy to treat breast cancer. We investigated how these particles were internalized by human breast cancer cells and which internalization routes resulted in the highest transfection efficacy. We identified that the major route of uptake for these PBAEs is caveolae-mediated endocytosis. The endocytosis mechanism that leads to the most efficient transfection varied with the polymer end-group and molecular weight. While clathrin-mediated endocytosis consistently led to an efficient transfection rate for all three polyplex types tested in this study, caveolae-mediated endocytosis became more important when the gene delivery polymer included the E7 end group or had higher molecular weight. We found that PBAE polyplex uptake more efficiently led to successful transfection when it was clathrin-mediated rather than caveolae-mediated. In certain circumstances (polymer 446L), caveolae-mediated uptake could be reduced dramatically while only marginally affecting transfection efficacy (a 61% reduction in uptake resulted in only an 8% reduction in transfection). This indicates that caveolae-mediated uptake may serve as a sink rather than a pathway to successful transfection for these particles. In order to optimize gene delivery with PBAE particles to human breast cancer, it is beneficial to use the 1-(3-aminopropyl)-4-methyl-piperazine (E7) end-group with a base polymer possessing higher overall molecular weight. These studies reveal for the first time that PBAEs can successfully transfect triple negative human breast cancer cells and that small differential changes to the same base polymer can lead to changes in the route of polyplex cellular uptake, even though polyplex biophysical properties remain constant.

ASSOCIATED CONTENT

Supporting Information

Supplementary data on chemical structures of all monomers and the NMR spectroscopy of representative PBAE polymers used in the study, the uptake and transfection of PBAE array, the optimization of endocytosis inhibitors, the correlation between % positive and the arithmetic/geometric mean of fluorescence intensity, and representative FACS plots. This material is available free of charge via the Internet at http://pubs.acs.org.

AUTHOR INFORMATION

Corresponding Author

*E-mail: green@jhu.edu. Telephone: 410-614-9113. Fax: 443-287-6298.

Notes

The authors declare no competing financial interest.

ACKNOWLEDGMENTS

J.K. thanks Samsung for a graduate scholarship. This project was supported in part by NIH grants R01EB016721 and R21CA152473. The authors thank the Microscopy and Imaging Core Module of the Wilmer Core Grant, EY001765. We would like to acknowledge Stephany Tzeng for providing some of the polymer samples.

ABBREVIATIONS

PBAE, poly(β-amino ester); PEI, poly(ethylenimine); CME, clathrin-mediated endocytosis; CvME, caveolae-mediated endocytosis; DLS, dynamic light scattering; NTA, nanoparticle tracking analysis

REFERENCES

(1) Verma, I. M., and Somia, N. (1997) Gene therapy – promises, problems and prospects. *Nature 389*, 239−42.
(2) Hollon, T. (2000) Researchers and regulators reflect on first gene therapy death. *Nat. Med. 6*, 6.
(3) Pack, D. W., Hoffman, A. S., Pun, S., and Stayton, P. S. (2005) Design and development of polymers for gene delivery. *Nat. Rev. Drug Discovery 4*, 581−93.
(4) Putnam, D. (2006) Polymers for gene delivery across length scales. *Nat. Mater. 5*, 439−51.
(5) Lynn, D. M., and Langer, R. (2000) Degradable poly(β-amino esters): synthesis, characterization, and self-assembly with plasmid DNA. *J. Am. Chem. Soc. 122*, 10761−10768.
(6) Green, J. J., Langer, R., and Anderson, D. G. (2008) A combinatorial polymer library approach yields insight into nonviral gene delivery. *Acc. Chem. Res. 41*, 749−59.
(7) Conner, S. D., and Schmid, S. L. (2003) Regulated portals of entry into the cell. *Nature 422*, 37−44.
(8) Marsh, M., and McMahon, H. T. (1999) The structural era of endocytosis. *Science 285*, 215−20.
(9) Takei, K., and Haucke, V. (2001) Clathrin-mediated endocytosis: membrane factors pull the trigger. *Trends Cell Biol 11*, 385−91.
(10) Wang, L. H., Rothberg, K. G., and Anderson, R. G. (1993) Mis-assembly of clathrin lattices on endosomes reveals a regulatory switch for coated pit formation. *J. Cell Biol. 123*, 1107−17.
(11) Pelkmans, L., and Helenius, A. (2002) Endocytosis via caveolae. *Traffic 3*, 311−20.
(12) Henley, J. R., Krueger, E. W., Oswald, B. J., and McNiven, M. A. (1998) Dynamin-mediated internalization of caveolae. *J. Cell Biol. 141*, 85−99.
(13) Pelkmans, L., Puntener, D., and Helenius, A. (2002) Local actin polymerization and dynamin recruitment in SV40-induced internalization of caveolae. *Science 296*, 535−9.
(14) Falcone, S., Cocucci, E., Podini, P., Kirchhausen, T., Clementi, E., and Meldolesi, J. (2006) Macropinocytosis: regulated coordination of endocytic and exocytic membrane traffic events. *J. Cell Sci. 119*, 4758−69.
(15) Amyere, M., Payrastre, B., Krause, U., Van Der Smissen, P., Veithen, A., and Courtoy, P. J. (2000) Constitutive macropinocytosis in oncogene-transformed fibroblasts depends on sequential permanent activation of phosphoinositide 3-kinase and phospholipase C. *Mol. Biol. Cell 11*, 3453−67.

(16) Bhise, N. S., Shmueli, R. B., Gonzalez, J., and Green, J. J. (2012) A novel assay for quantifying the number of plasmids encapsulated by polymer nanoparticles. *Small 8*, 367−73.
(17) Green, J. J. (2012) 2011 Rita Schaffer lecture: nanoparticles for intracellular nucleic acid delivery. *Ann. Biomed. Eng. 40*, 1408−18.
(18) Shmueli, R. B., Sunshine, J. C., Xu, Z., Duh, E. J., and Green, J. J. (2012) Gene delivery nanoparticles specific for human microvasculature and macrovasculature. *Nanomedicine 8*, 1200−7.
(19) Sunshine, J. C., Sunshine, S. B., Bhutto, I., Handa, J. T., and Green, J. J. (2012) Poly(β-amino ester)-nanoparticle mediated transfection of retinal pigment epithelial cells in vitro and in vivo. *PLoS One 7*, e37543.
(20) Tzeng, S. Y., Guerrero-Cazares, H., Martinez, E. E., Sunshine, J. C., Quinones-Hinojosa, A., and Green, J. J. (2011) Non-viral gene delivery nanoparticles based on poly(β-amino esters) for treatment of glioblastoma. *Biomaterials 32*, 5402−10.
(21) Tzeng, S. Y., and Green, J. J. (2013) Subtle changes to polymer structure and degradation mechanism enable highly effective nanoparticles for siRNA and DNA delivery to human brain cancer. *Adv. Healthcare Mater. 2*, 468−80.
(22) Tzeng, S. Y., Hung, B. P., Grayson, W. L., and Green, J. J. (2012) Cystamine-terminated poly(beta-amino ester)s for siRNA delivery to human mesenchymal stem cells and enhancement of osteogenic differentiation. *Biomaterials 33*, 8142−51.
(23) Green, J. J., Zugates, G. T., Tedford, N. C., Huang, Y. H., Griffith, L. G., Lauffenburger, D. A., Sawicki, J. A., Langer, R., and Anderson, D. G. (2007) Combinatorial modification of degradable polymers enables transfection of human cells comparable to adenovirus. *Adv. Mater. 19*, 2836.
(24) Anderson, D. G., Akinc, A., Hossain, N., and Langer, R. (2005) Structure/property studies of polymeric gene delivery using a library of poly(beta-amino esters). *Mol. Ther. 11*, 426−34.
(25) Sunshine, J., Green, J. J., Mahon, K., Yang, F., Eltoukhy, A., Nguyen, D. N., Langer, R., and Anderson, D. G. (2009) Small molecule end groups of linear polymer determine cell-type gene delivery efficacy. *Adv. Mater. 21*, 4947−4951.
(26) Sunshine, J. C., Akanda, M. I., Li, D., Kozielski, K. L., and Green, J. J. (2011) Effects of base polymer hydrophobicity and end-group modification on polymeric gene delivery. *Biomacromolecules 12*, 3592−600.
(27) Sunshine, J. C., Peng, D. Y., and Green, J. J. (2012) Uptake and transfection with polymeric nanoparticles are dependent on polymer end-group structure, but largely independent of nanoparticle physical and chemical properties. *Mol. Pharm. 9*, 3375−83.
(28) Zugates, G. T., Tedford, N. C., Zumbuehl, A., Jhunjhunwala, S., Kang, C. S., Griffith, L. G., Lauffenburger, D. A., Langer, R., and Anderson, D. G. (2007) Gene delivery properties of end-modified poly(beta-amino ester)s. *Bioconjugate Chem. 18*, 1887−96.
(29) Brey, D. M., Erickson, I., and Burdick, J. A. (2008) Influence of macromer molecular weight and chemistry on poly(beta-amino ester) network properties and initial cell interactions. *J. Biomed. Mater. Res. A 85*, 731−41.
(30) Rejman, J., Oberle, V., Zuhorn, I. S., and Hoekstra, D. (2004) Size-dependent internalization of particles via the pathways of clathrin- and caveolae-mediated endocytosis. *Biochem. J. 377*, 159−69.
(31) Harush-Frenkel, O., Debotton, N., Benita, S., and Altschuler, Y. (2007) Targeting of nanoparticles to the clathrin-mediated endocytic pathway. *Biochem. Biophys. Res. Commun. 353*, 26−32.
(32) Shmueli, R. B., Bhise, N. S., and Green, J. J. (2013) Evaluation of Polymeric Gene Delivery Nanoparticles by Nanoparticle Tracking Analysis and High-throughput Flow Cytometry. *J Vis Exp. 73*, e50176.
(33) Iversen, T. G., Skotland, T., and Sandvig, K. (2011) Endocytosis and intracellular transport of nanoparticles: present knowledge and need for future studies. *Nano Today 6*, 176−185.
(34) Rejman, J., Bragonzi, A., and Conese, M. (2005) Role of clathrin- and caveolae-mediated endocytosis in gene transfer mediated by lipo- and polyplexes. *Mol. Ther. 12*, 468−74.
(35) van der Aa, M. A., Huth, U. S., Hafele, S. Y., Schubert, R., Oosting, R. S., Mastrobattista, E., Hennink, W. E., Peschka-Suss, R., Koning, G. A., and Crommelin, D. J. (2007) Cellular uptake of cationic polymer-DNA complexes via caveolae plays a pivotal role in gene transfection in COS-7 cells. *Pharm. Res. 24*, 1590−8.
(36) Ivanov, A. I. (2008) Pharmacological inhibition of endocytic pathways: is it specific enough to be useful? *Methods Mol. Biol. 440*, 15−33.
(37) dos Santos, T., Varela, J., Lynch, I., Salvati, A., and Dawson, K. A. (2011) Effects of transport inhibitors on the cellular uptake of carboxylated polystyrene nanoparticles in different cell lines. *PLoS One 6*, e24438.
(38) Singh, R. D., Puri, V., Valiyaveettil, J. T., Marks, D. L., Bittman, R., and Pagano, R. E. (2003) Selective caveolin-1-dependent endocytosis of glycosphingolipids. *Mol. Biol. Cell 14*, 3254−65.
(39) Saeed, M. F., Kolokoltsov, A. A., Albrecht, T., and Davey, R. A. (2010) Cellular entry of ebola virus involves uptake by a macropinocytosis-like mechanism and subsequent trafficking through early and late endosomes. *PLoS Pathog. 6*, e1001110.
(40) Luhmann, T., Rimann, M., Bittermann, A. G., and Hall, H. (2008) Cellular uptake and intracellular pathways of PLL-g-PEG-DNA nanoparticles. *Bioconjugate Chem. 19*, 1907−16.
(41) Bhise, N. S., Gray, R. S., Sunshine, J. C., Htet, S., Ewald, A. J., and Green, J. J. (2010) The relationship between terminal functionalization and molecular weight of a gene delivery polymer and transfection efficacy in mammary epithelial 2-D cultures and 3-D organotypic cultures. *Biomaterials 31*, 8088−96.
(42) Bishop, C. J., Ketola, T.-M. C., Tzeng, S. Y., Sunshine, J. C., Urtti, A. O., Lemmetyinen, H., Vuorimaa-Laukkanen, E., Yliperttula, M., and Green, J. J. (2013) The effect and role of carbon atoms in poly(beta-amino ester)s for DNA binding and gene delivery. *J. Am. Chem. Soc. 135*, 6951−7.